INVESTIGATION OF SOLDER JOINT RELIABILITY THROUGH IMPACT FATIGUE LOADING

Brian Roggeman and Martin Anselm
Unovis Solutions
Binghamton, NY

Pradosh Guruprasad and James Pitarresi
Mechanical Engineering Dept., Binghamton University
Binghamton, NY

ABSTRACT

The most common reliability concern in portable electronic devices is that of mechanical loading caused by physical handling. In these mechanical loading situations, solder joint failure may occur either in the first impact, or after repeated loadings. Intermetallic fracture is a common failure mode in these events due to the high strain rate experienced within the solder. As strain rate increases, so do both solder stiffness and strength, which then transfers more stress to the bonds. Solder joint shear and pull testing are routinely used to evaluate the solder joint on the package level, however these methods do not currently simulate repeated high strain rate impact loading that occurs during repeated drop testing, for example.

A pendulum impact tester has been developed for investigating not just the ultimate impact strength, but more importantly the repeated impact reliability of individual solder joints. The pendulum impact test is essentially an input-energy controlled shear test. The important characteristics of the system are the pendulum length, mass and release angle. By limiting the pendulum mass and maximizing the release angle, very high strain rates can be produced, with relatively low input energy, and the test can be conducted repeatedly until failure.

SAC305 solder balls were populated on a surface finish of either organic solderability preservative (OSP) or Electroless Nickel-Immersion Gold (ENIG). The different intermetallic layer formation of these surface finishes provides for vastly different drop/impact reliability that is not clearly depicted in strength measurements.

The relationship between impact energy and cycles to failure for each finish was determined, indicating a difference in behavior between OSP and ENIG, as well as a strong correlation to degradation during thermal aging. The impact fatigue testing on individual solder balls shows a stronger comparison to drop testing than just shear strength testing. The ultimate strength and the resistance to impact fatigue loading are not necessarily correlated.

Keywords: lead-free solder, drop, impact, intermetallic.

INTRODUCTION

With the transition to lead-free soldering and the popularity of portable electronic devices, solder joint reliability can no longer be described solely by thermal cycling. Mechanical shock loads, such as those experienced from dropping a cell phone for example, induce stresses at very high strain rates. Solder is known to be a highly strain rate dependent material, and both the stiffness and ultimate tensile strength increase with increasing strain rate. The result is that slow speed testing cannot be used as a replacement for high speed testing. The combination of high strain rates and increased solder stiffness from Pb-free solders increases the chances for brittle failure modes, such as intermetallic fracture and pad cratering.

Considering intermetallics, we may be concerned with different surface finishes and various degradation mechanisms that are likely to occur during the lifecycle of the product. For example, ENIG may be plagued by “black pad” issues that cause very early failures, while soldering to copper may be very sensitive to Kirkendall voiding that occurs after extended thermal exposure [1]. Implementing screening tests is becoming an important step in the development of a product.

Board level testing, such as the JEDEC Board Level Drop Test Method [2], is meant to account for the worst-case scenario, but is very expensive both in terms of test costs and test time. Full board assemblies must be produced for testing. Taking advantage of board symmetry, only a few components per board will experience the same response, and will be directly comparable. From those, failure is typically defined as the first electrical discontinuity, which is usually related to a single “critical” solder joint. This will result in only a few joints per assembly being tested at a time. In comparison, solder ball testing can be done on a single BGA device, and several hundred to thousands of solder balls are available for testing. This is important for developing proper statistical analysis, and finding outliers that may not show up in the limited sample set from board level testing.

BACKGROUND

Because of the high cost and time commitments involved in drop testing, it is highly desirable to develop alternative testing procedures that generate similar rankings and results. Numerous researchers have investigated different techniques including finite element modeling, solder ball pull, shear and impact testing.

There have been several attempts at correlating individual solder ball testing to board level drop test failures. Slower speed ball tests fail to simulate the strain rates seen in drop testing, and therefore provide for poor correlations. Chiu, et al. studied the effect of aging and formation of Kirkendall voiding on drop testing, and found that strength testing alone does not correlate to the reduction in drop test reliability. Instead, they found that the percentage of brittle fracture gave a better indication of the degradation of the IMC layer robustness [3]. Higher speed solder ball testing can better simulate drop test strain rates, yet correlations between failure rate and strength have still proven to be weak. Wong, et al. used a micro-impact tester to generate high strain rates, and investigated different testing configurations. They concluded that strength, even at similar strain rates as drop, did not correlate to drop test failures. Rather, energy or solder joint ductility gave a better comparison [4]. Ou, et al. used a pendulum impact tester to measure impact toughness on Ni/Au substrates, but not as a function of repeated loadings. Their findings indicated that failure energy was highly dependent on alloy composition and thermal aging times [5]. Johnson et al. used high speed testing and found some similarities between the trends of board level drop test and the percentage of brittle fractures in solder-ball testing [6]. Song, et al presented very promising correlation curves between high speed solder ball testing and drop reliability. Their data included brittle fracture percentage, strength and fracture energy correlations using both OSP and ENIG surface finishes [7].

In all the cases above, only a single overstress was considered as the correlation factor to repeated drop reliability. Because drop testing is usually a repeated loading condition, ultimate strength testing can only accurately represent the loading rate, without addressing the crack propagation properties of the material. Testing for pad cratering has shown a much better correlation to drop testing when done in fatigue mode rather than strength mode [8]. The following addresses both the loading rate as well as crack propagation.

EXPERIMENTAL SETUP

Test Vehicles

The test vehicles used in this study are 256 I/O component substrates (Figure 1). The substrate is 16-mil thick FR4, with solder-mask-defined (SMD) pads with 23-mil mask openings. 750 micron SAC305 solder balls were attached using a tacky flux and reflowed at 245 °C in an environment with less than 50 ppm O_2. Thermal aging was performed in batch ovens at 100 °C and 125 °C.

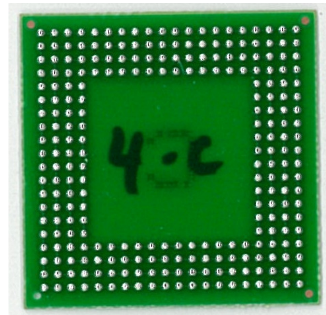

Figure 1. Test vehicle substrate.

Test Apparatus

A pendulum impact tester was developed for the testing of individual solder balls. Pendulum impact has the advantage of high strain rates with relatively low impact energy, which lends itself well to repeated impact loading resulting in crack propagation rather than ultimate strength failures.

The tester developed for this investigation uses a Pasco Scientific rotary sensor mounted to a rigid structure. The accuracy of the sensor is +/- 0.09°. Digital data acquisition software captures the real time angle, angular velocity and angular acceleration with a maximum sample rate of 1000 Hz. The testing presented here used a sample rate of 40 Hz.

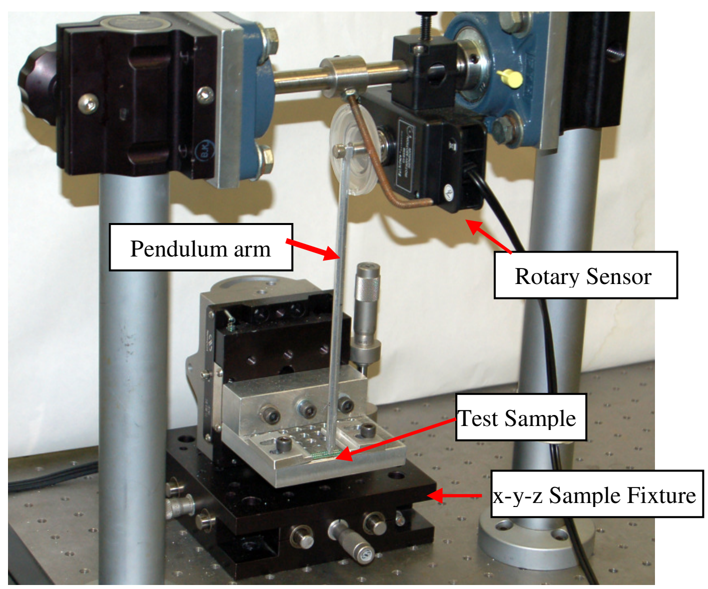

Figure 2. Pendulum Testing Apparatus

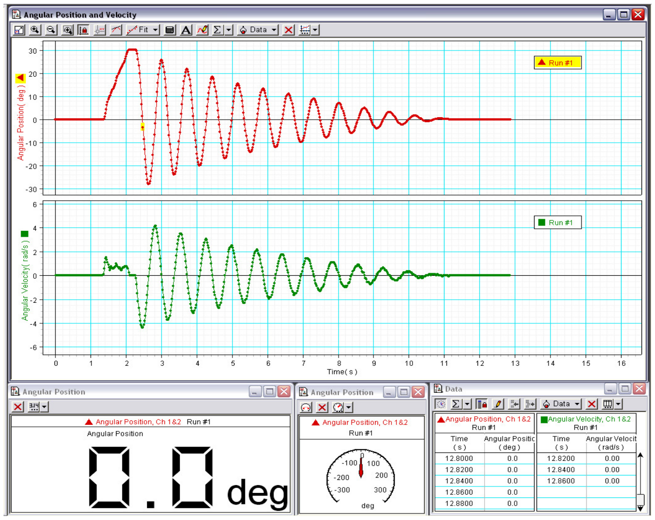

Figure 3. Graphical output of angular position (top) and angular velocity (bottom) for a free swing. Pendulum comes to rest at 0 deg.

The pendulum arm was constructed from aluminum to reduce the mass, and used a ‘T’ cross section which increases the stiffness and minimizes rod flexure during impact. The impact tip of the rod is machined flat and the sides tapered down to 800 microns so that it would only impact a single solder ball at time (Figure 4).

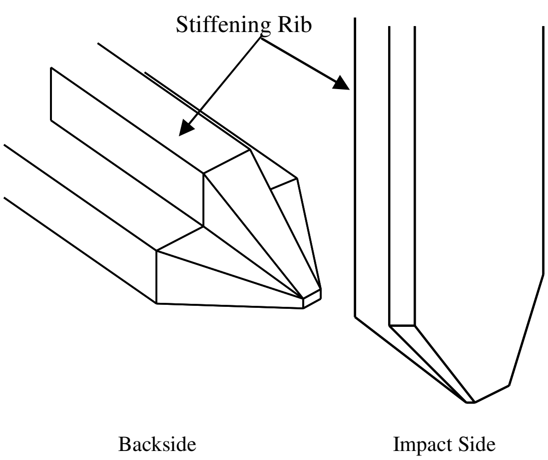

Figure 4. Diagram of pendulum arm detail.

A rigid pendulum can be modeled as a simple pendulum through the use of a modified length term in the pendulum equations of motion. The modified length is described as

$$L = J/(m*a), \tag{1}$$

where L is the modified or effective length, J is the moment of inertia of the pendulum arm about the axis of rotation, m is the mass and a is the distance between the rotation axis and the center of gravity of the pendulum arm [9]. The center of mass of our pendulum, a, was found to be 91.53 mm from the axis of rotation. The resulting effective length is then 116 mm.

The impact velocity was measured as a function of release angle. Here we define the impact velocity as the linear velocity of the pendulum tip, at an angle of zero which corresponds to impact at the lowest point in the pendulum arc. Figure 5 shows a graphical representation of the linear impact velocity versus release angle. This system can achieve up to 2.28 m/s impact velocity at 90° release angle.

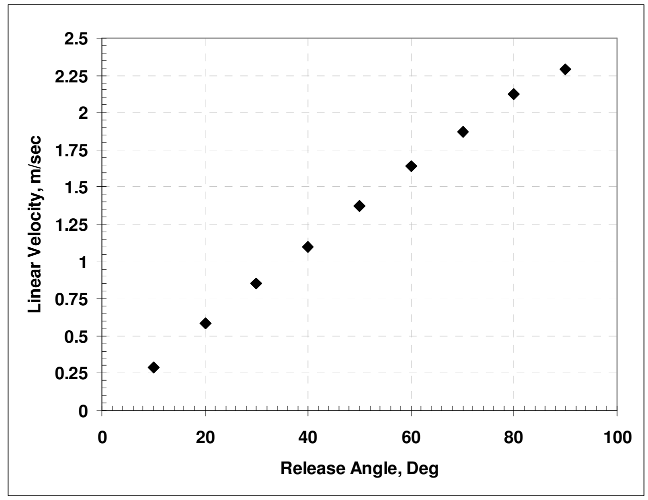

Figure 5. Measured linear velocity versus release angle.

Loading energy is proving to be an important metric in mechanical failures [10]. The predicted impact energy at any release angle can be approximated by invoking the conservation of energy principal. The potential energy at release is equal to the kinetic energy at impact, if impact occurs when the pendulum is at its lowest point. Impact energy is then given by

$$E_{impact} = mga(1-\cos(\theta)). \tag{2}$$

Measured impact energy is calculated from the measured angular velocity and moment of inertia. The equation is given as

$$E_{impact} = ½\, J\omega^2 \tag{3}$$

where ω is the angular velocity. Both the predicted and measured impact energy is shown in Figure 6, indicating that there is some loss due to friction. For small release angles the predicted energy is close to the actual energy, but the error grows with larger release angles. Depending on the release angle used in testing, conservation of energy may not be suitable to predict impact energy. This plot is used to determine our impact energy for the following testing.

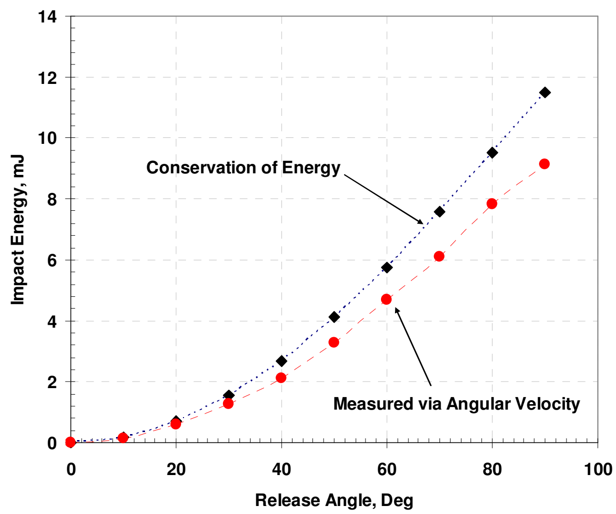

Figure 6. Impact energy versus release angle, using conservation of energy and calculation based on velocity.

RESULTS

The motivation behind the development of micro-impact fatigue comes from the variation of intermetallic layer robustness, especially when different finishes and degradation mechanisms are considered. For example, it has now been well documented that the drops test performance when using ENIG is generally inferior to OSP. To illustrate this, drop testing was carried out according to the procedures in the JEDEC JESD22-B111 standard [2]. The PCB finish was OSP, while the components were either OSP or ENIG, and the solder alloy was SAC305. In-situ event detection was used to monitor for failure, and the drops to fail was recorded. A total of 18 components were tested for each condition.

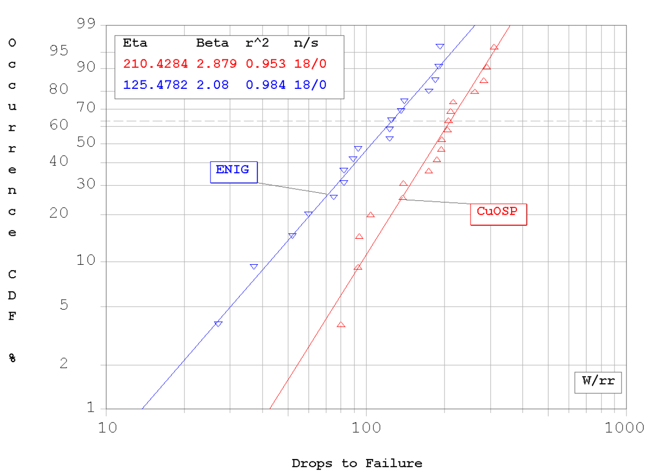

Figure 7. Drop test results of OSP and ENIG components.

Figure 7 shows a 2-parameter Weibull fit of the reliability of each component surface finish. The characteristic life, which corresponds to when 63.2% of the population has failed, is indicated by the Eta value. For this particular test vehicle, the OSP component almost doubles the lifetime of the ENIG component, with characteristic lifetimes given by 210 and 125 drops, respectively. The failure modes are shown in Figure 8. Both systems fail by fracture at the component side intermetallic layer. The OSP finish shows a crack through the Cu_6Sn_5 layer, while the ENIG finish shows cracks both within the Ni_3Sn_4 layer and along the interface with the copper pad.

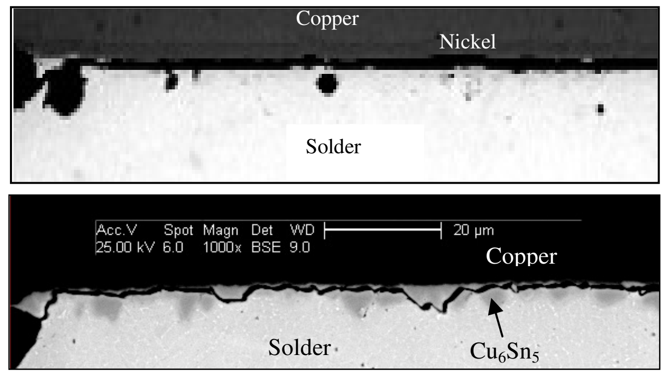

Figure 8. Failure mode seen on ENIG (top) and OSP (bottom) in drop testing.

Effect of Thermal Aging

Isothermal aging was used to investigate changes in intermetallic behavior. It is widely known that elevated temperatures cause the intermetallic layers to grow at rates governed by Fick's Law [11]. The intermetallic structures for these substrates were investigated to better understand the intermetallic conditions used in this test.

Intermetallic growth rates for lead-free solder on Ni has been shown to be very slow particularly at the 100ºC temperature [12]. Therefore we did not expect to see a dramatic increase in the intermetallic thicknesses in these samples. We did not observe any issues with the formation of these intermetallics, so black pad was not present, and we can assume that the results of the impact testing are representative of a standard intermetallic formation on ENIG. Figures 9 and 10 show examples of joints on ENIG after thermal aging and solder etching.

Cu intermetallic formation also grows on average as well as becoming smoother over time during the isothermal aging at 100ºC and 125ºC. The Cu substrate also exhibited the formation of Kirkendall voiding within the Cu_3Sn layer that occurs after extended thermal exposure [1]. This may have affected the Cu intermetallic growth rates. Kirkendall voiding has been seen to contribute to reliability issues in high strain rate loading [3]. Figures 11 and 12 show examples of joints on Cu OSP, after thermal aging and solder etching. Figure 13 shows voiding on an unetched sample after 2 weeks at 125 °C.

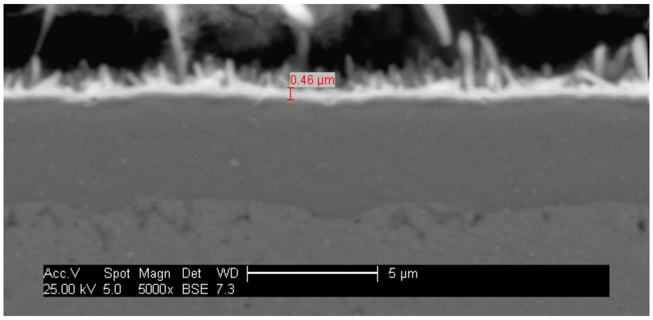

Figure 9. 125°C 100 hours of aging on Ni-P substrate

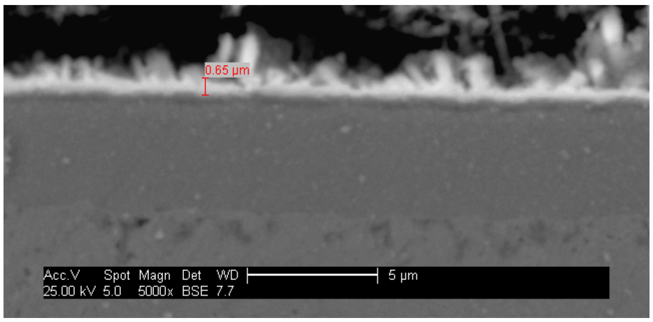

Figure 10. 125°C 300 hours of aging on Ni-P substrate

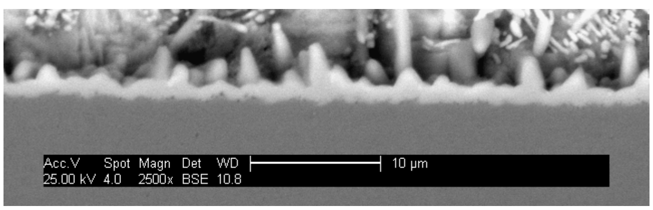

Figure 11. 125°C 100 hours of aging on Cu substrate

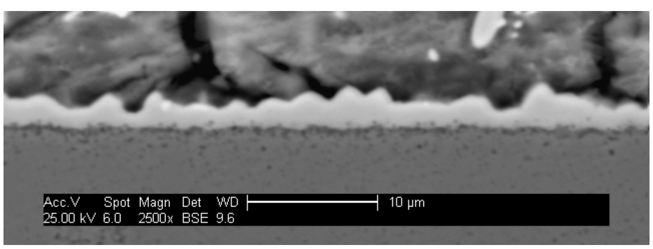

Figure 12. 125°C 300 hours of aging on Cu substrate

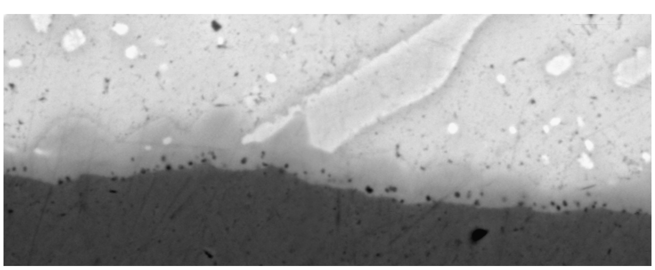

Figure 13. Voiding seen Cu_3Sn in after 2 weeks at 125 °C. 4000X magnification.

Initial Test Parameters

Initial trials were run to determine the preferred input angle and corresponding input energy. Because the system requires manual intervention in terms of resetting the pendulum arm after each impact, the goal was to fail within a reasonable cycle time, while still producing a failure mode within the intermetallic layer. A total of twelve solder joints were tested for each condition.

The initial evaluation included pendulum release angles of 30° and 40°, which corresponds to impact velocities of 0.85 m/s and 1.10 m/s, respectively, and impact energies of 1.27 mJ and 2.12 mJ, respectively. Figure 14 shows a 2-parameter Weibull comparison of brittle failures occurring on OSP surface finish for both the 30° and 40° release angles. Figure 15 shows the same comparison on the ENIG surface finish. The characteristic lifetime is indicated by the Eta value.

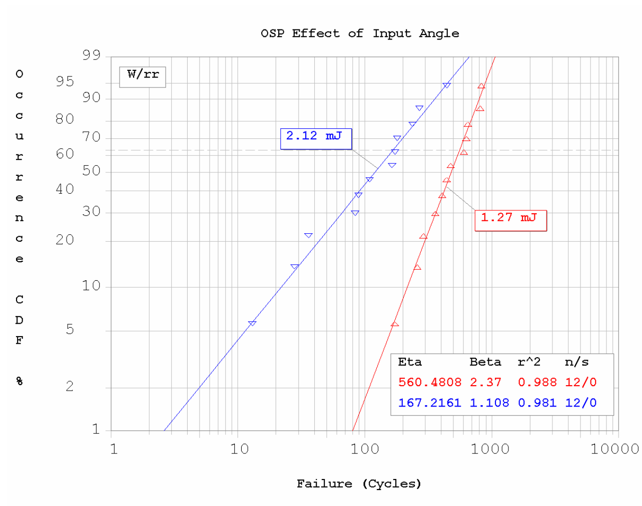

Figure 14. Impact energy dependence on IMC failures on OSP.

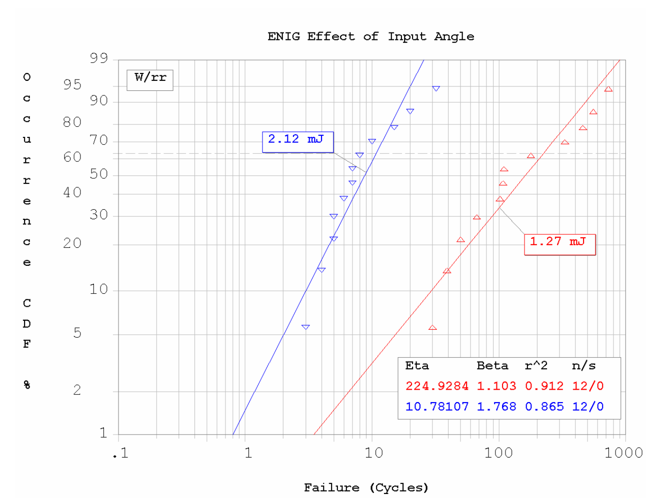

Figure 15. Impact energy dependence for IMC failures on ENIG.

From the results above, a 40° pendulum release angle, corresponding to an impact velocity of 1.10 m/s and an impact energy of 2.12 mJ was selected for the remainder of the testing. This produced mostly intermetallic failures, while keeping the test time reasonable and cycles to failure within the same range that would be expected in drop testing. The time-zero comparison between OSP and ENIG is shown in Figure 16. In this case, the characteristic lives of the intermetallics on OSP and ENIG are 167 and 10 cycles, respectively. This represents a difference of over 16X.

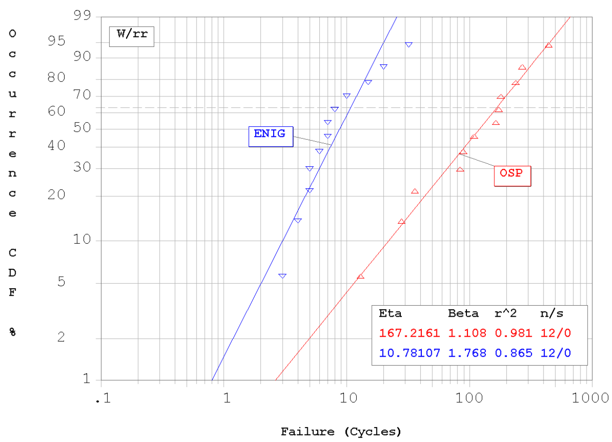

Figure 16. IMC lifetime comparison of OSP and ENIG.

Comparatively, cold-bump pull (CBP) testing was used to determine the strength of the IMC layers on both surface finishes. A pull speed of 5mm/s was used, which has been shown to be successful at correlating to drop test failures [7], using either brittle fracture percentage or fracture energy as the correlation metric. Figure 17 shows the average strength and brittle fracture percentage for both OSP and ENIG at time-zero. The average strength was statistically equivalent for both surface finishes, at approximately 2950 grams-force. The difference in brittle fracture percentage highlights that the ENIG IMC layer is more prone to fracture than the IMC layer on OSP. However, the difference is only 20% between the two finishes. Comparatively, micro-impact fatigue testing provides a much more clear distinction between these two finishes.

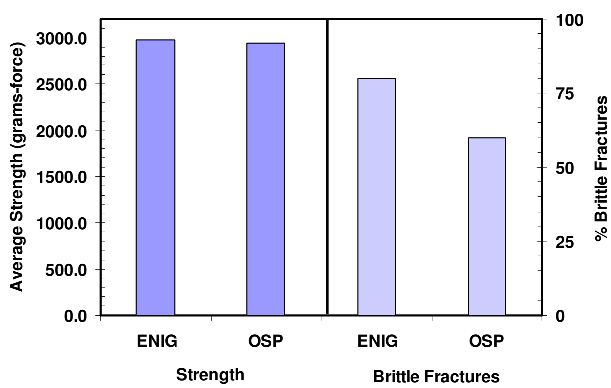

Figure 17. Strength and Brittle Fracture Percent for pull-strength testing.

Micro-Impact fatigue was conducted on the same substrates to observe changes in behavior through thermal aging at 100 °C and 125 °C over a period of 500 hours. Testing was carried out at selected time intervals. Figure 18 shows a compilation of this data, plotting the mean time to failure (MTF) versus aging time for each pad finish.

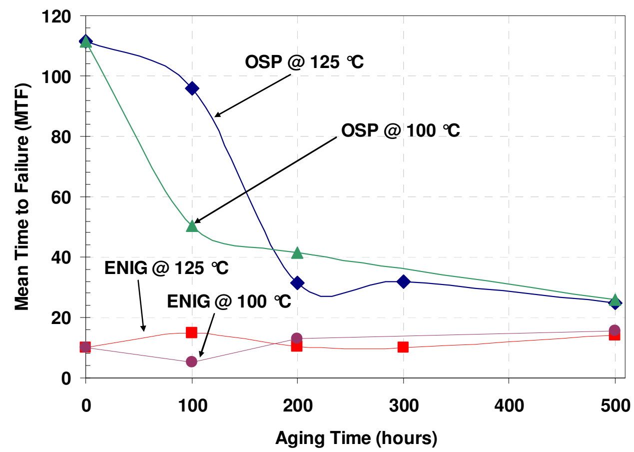

Figure 18. Mean time to failure for intermetallic fracture on each pad finish at different aging temperatures.

The plot above shows that OSP degrades in cycles to failure much quicker than ENIG does. The behavior is consistent with the difference in IMC growth rates between Cu and Ni intermetallics. There does not appear to be much temperature dependence with either finish, either than the difference at 100 hours. During aging, the intermetallic layers grow thicker, but the solder softens as the smaller particles are drained out into larger precipitates. Softer solder can absorb more of the impact energy. The difference seen here may be due to this competing effect. However, past 100 hours, the degradation in intermetallic robustness dominates. Both the IMC growth and Kirkendall voiding contribute to the degradation on Cu, while only the growth mechanism contributes to the degradation on Ni.

Failure modes were examined for the different aging conditions. All IMC failures included some portion of bulk solder failure on the opposite side of the pad from the loading direction. This is attributed to the crack propagating through the IMC, which eventually causes a "solder hinge" towards the end of the crack growth. Because of the moment applied at this hinge at the end of the crack growth, it causes this small amount of solder to ultimately fail. This type of failure mode is not typically seen in drop testing because there is a reaction moment from the component that resists the free rotation of the solder joint.

Failure on ENIG occurred both through the Ni_3Sn_4 and at the Ni pad interface, for all aging conditions. Failure on OSP occurred through the Cu_6Sn_5 layer at time zero, but began to transition to the interface between the Cu_6Sn_5 layer and the Cu_3Sn layer. After 500 hours at 125 °C, we see the Cu_3Sn layer and evidence of Kirkendall voiding near the fracture surface.

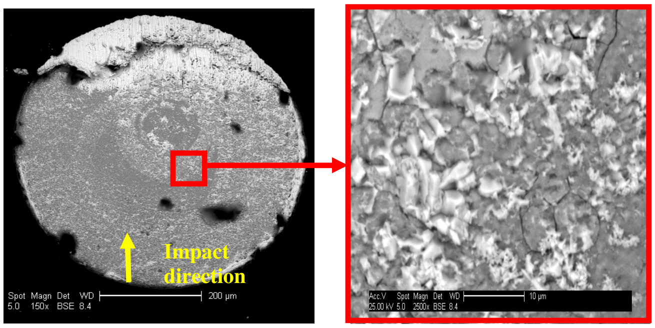

Figure 19. Pad surface after impact-fatigue on ENIG at 0 hrs. Both Ni_3Sn_4 IMC and Ni surface are visible.

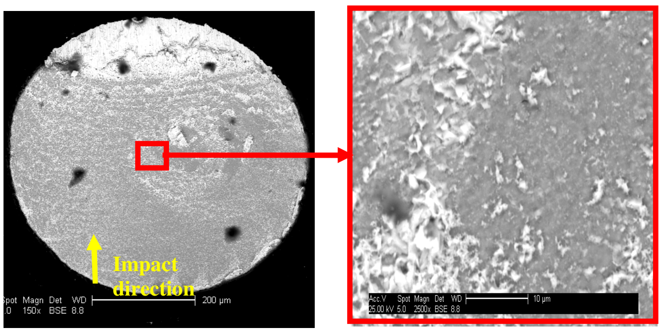

Figure 20. Pad surface after impact-fatigue on ENIG at 500 hrs. at 125 °C. Ni_3Sn_4 IMC and Ni surface are visible.

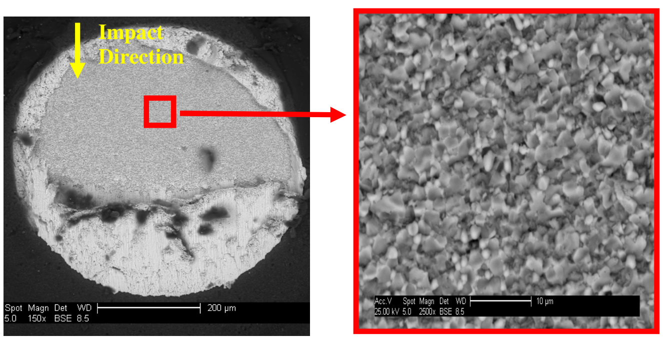

Figure 21. Pad surface after impact-fatigue on OSP at 0 hrs. Only Cu_6Sn_5 IMC is visible.

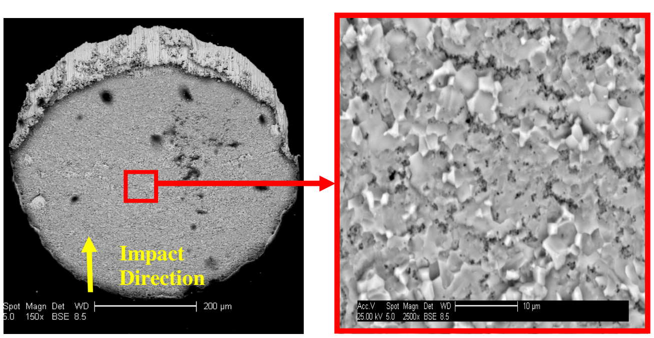

Figure 22. Pad surface after impact-fatigue on OSP at 500 hrs. at 125 °C. Cu_6Sn_5 and Cu_3Sn IMC structures are visible, as well as small voids within the Cu_3Sn.

Cold bump pull testing was used to complement the pendulum impact testing. Only the 125 °C aging condition was considered. Twenty solder joints were tested for each condition, using a pull speed of 5 mm/sec. The average strength is shown in Figure 23 for both finishes and aging times up to 500 hours.

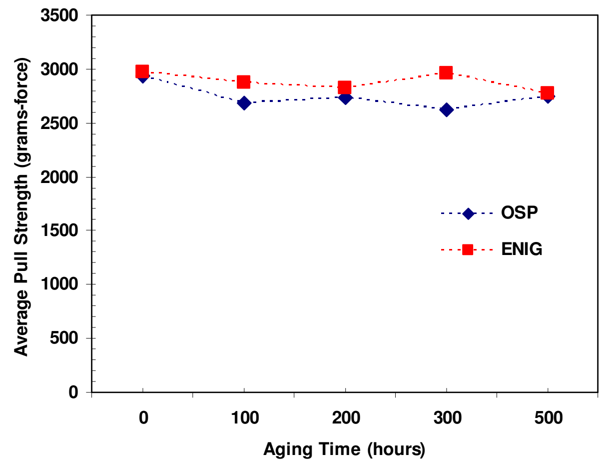

Figure 23. Average Pull Strength using Cold Bump Pull method.

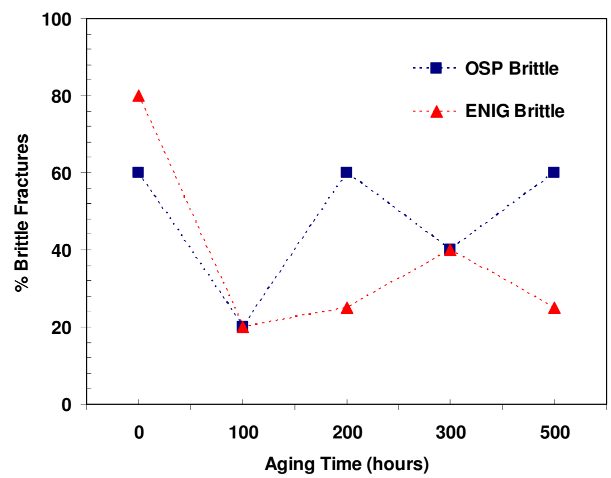

Figure 24. % Brittle Fractures vs. Aging time at 125 °C during cold-bump pull testing.

Comparing the CBP data, both in terms of strength and % Brittle Fractures, to the micro-impact fatigue data, there appears to be little correlation. There is some amount of strength reduction in the OSP samples, but that amounts to only an 11% reduction. In terms of brittle fracture percentage, we can see evidence of solder softening at 100 hours, as both ENIG and OSP exhibit the fewest brittle fractures at this aging time. Both surface finishes then increase in brittle fractures under continued aging as the IMC layers being to weaken. Again, we see a larger change in the OSP due to the slow growth rates experienced in the Ni IMC.

CONCLUSIONS

A micro-impact tester was developed to perform high strain-rate fatigue measurements on individual solder balls. This has proven to be an important complement to high speed strength measurements as it provides for crack propagation measurements that are not accurately simulated with single strength measurements. A repeated loading condition may not always correlate with a single overstress. Because of this, impact-fatigue testing is a more general test than high speed strength testing.

Surface finishes of OSP and ENIG were analyzed as a first illustration of this technique. Repeated drop testing has shown that these two finishes perform significantly different. Strength measurements alone may not be discriminating enough to generate useful comparisons. In our case, the strength difference was negligible, yet drop test performance was different by a factor of 2. Micro-impact fatigue testing showed that there was indeed a large difference in the crack propagation properties of these two finishes.

Thermal aging was used to modify the behavior of the IMC layers on both finishes. This is a typical test that accelerates expected use conditions. It was found that the solder tends to soften during thermal aging, as smaller IMC particles are drained into larger precipitates. The competing effects of solder softening and IMC growth/degradation make it difficult to generalize the results just for IMC degradation. Increasing the strain rate or impact velocity may overcome the solder softening effect so that only the IMC layer behavior is being measured. Further developmental work is underway to better correlate the impact energy and strain rate with that experienced in a board level loading condition. This testing technique may have a critical role as a screening procedure on incoming product to address quality concerns.

REFERENCES

[1] P. Borgesen, L. Yin, P. Kondos, D. Henderson, G. Servis, J. Wang, K. Srihari, "Sporadic Degradation in Board Level Drop Reliability - Those Aren't All Kirkendall Voids!", ECTC 2007, pp. 136-146.

[2] JEDEC Standard JESD22-B111, Board Level Drop Test Method of Components for Handheld Electronic Products, 2003.

[3] T-C Chiu, K. Zeng, R. Stierman, D. Edwards, K. Ano, "Effect of Thermal Aging on Board Level Drop Reliability for Pb-Free BGA Packages", ECTC 2004, pp. 1256-1262.

[4] E.H. Wong, Y-W Mai, R. Rajoo, K.T. Tsai, F. Liu, S.K.W. Seah, C-L Yeh, "Micro Impact Characterisation of Solder joint for Drop Impact Application", 2006 ECTC, pp 64-71.

[5] S. Ou, Y. Xu, K.N. Tu, "Micro-Impact Test on Lead-Free BGA Balls on Au/ElectrolyticNi/Cu Bond Pad", ECTC2006, pp. 467-471.

[6] M. Johnson, H. Lu, D. Lawhead, T. Tessier, D. Scott, A. Curtis, "Using High Speed Shear and Cold Ball Pull to Characterize Lead Free Solder Alloys and Predict Board Level Drop Test Performance", ECTC 2007, pp. 536-542.

[7] F. Song, S.W. Ricky Lee, K. Newman, B. Sykes, S. Clark, "Brittle Failure Mechanism of SnAgCu and SnPb Solder Balls during High Speed Ball Shear and Cold Ball Pull Tests", ECTC 2007, pp. 364-372.

[8] B. Roggeman, P.Borgesen, J. Li, G. Godbole, P. Tumne, K. Srihari, T. Levo, J. Pitarresi, "Assessment of PCB Pad Cratering resistance by Joint Level Testing", ECTC 2008. pp. 884-892.

[9] E.I. Butikov, "The Rigid Pendulum – an Antique but Evergreen Physical Model", European Journal of Physics, Vol. 20, No. 5, 1999, pp. 429-441.

[10] F. Mirza, B. Roggeman, J. Pitaressi, "Investigation of Impact Response of Pb-Free Assemblies and Comparison of Drop Test with Cyclic 4-Point Bend", Society of Experimental Mechanics XI International Congress, June 2008.

[11] Li, G Y., and B L. Chen. "Formation and Growth Kinetics of Interfacial Intermetallics in Pb-Free Solder Joint." IEEE TRANSACTIONS ON COMPONENTS AND PACKAGING TECHNOLOGIES Vol. 26 No. 3 (2003): pp. 651-58.

[12] Xu, Luhua, John H. Pang, Kithva H. Prakash, and T H. Low. "Isothermal and Thermal Cycling Aging on IMC Growth Rate in Lead-Free and Lead-Based Solder Interface." IEEE TRANSACTIONS ON COMPONENTS AND PACKAGING TECHNOLOGIES Vol. 28 No.3 (2005): pp. 408-14.